Modelling of Hybrid Scenario: from present-day experiments toward ITER

X. Litaudon[1], I. Voitsekhovitch[2], J.F. Artaud[1], P. Belo[3], J.P.S. Bizarro[3], T Casper[4], J. Citrin[5], E. Fable[6], J. Ferreira[3], J. Garcia[1], L. Garzotti[2], G. Giruzzi[1] , J. Hobirk[6], G.M.D. Hogeweij[5], F. Imbeaux[1], E. Joffrin[1], F. Koechl[7], F. Liu[1], J. Lönnroth[8], D. Moreau[1], V. Parail[2], P.B. Snyder[9], M. Schneider[1], ASDEX Upgrade Team, JET-EFDA contributors*, and the EU-ITM ITER Scenario Modelling group

[1]CEA, IRFM, F-13108 Saint Paul Lez Durance, France
[2]EURATOM/CCFE Fusion Association, Culham Science Centre, Abingdon OX14 3DB UK
[3]Associacão EURATOM-IST, Instituto de Plasmas e Fusão Nuclear, Lisbon, Portugal
[4]ITER Organization, F-13115 Saint Paul lez Durance, France
[5]FOM Institute DIFFER—Dutch Institute for Fundamental Energy Research, Association EURATOM-FOM, Nieuwegein, The Netherlands
[6]Max-Planck-Institut für Plasmaphysik, EURATOM-Assoziation, Garching, Germany
[7]Association EURATOM-ÖAW/ATI, Atominstitut, TU Wien, 1020 Vienna, Austria
[8]Helsinki University of Technology, Association EURATOM-Tekes, P.O.Box 4100, FIN-02015 TKK, Finland
[9]General Atomics, San Diego, USA
*See the Appendix of F. Romanelli et al., Proceedings of the 24th IAEA Fusion Energy Conference 2012, San Diego, USA

- The 'hybrid' scenario is an attractive operating scenario for ITER since it combines long plasma duration with the reliability of the reference H-mode regime.
- We review the recent European modelling effort carried out within the ITER Scenario Modelling (ISM) working group (ISM-WG is organized within the EFDA Task Force on Integrated Tokamak Modelling ITM-TF [1, 2]) :
  - (i) understanding the underlying physics of the hybrid regime in ASDEX-Upgrade and JET
  - (ii) extrapolating them toward ITER

Integrated modeling of ASDEX-Upgrade and JET hybrid scenario

JET and ASDEX-Upgrade database

- More than fourteen JET and two ASDEX-Upgrade hybrid scenarios performed under different experimental conditions have been simulated in an interpretative and predictive
- By optimising the current density profile $H_{IPB98(y,2)}$ up to of 1.4.
- JET : q-profile modification via the 'current-overshoot' method [2, 3].
- ASDEX-Upgrade: q-profile modification by varying the NBI timing, with the later heating case resulting in a broader q-profile [4]

Current diffusion interpretative analysis

- neo-classical prediction for the resistivity and bootstrap current interpretative analysis
- same modelling assumption with CRONOS [5] for JET & ASDEX-Upgrade
- JET : dynamics is reasonably well reproduced
- ASDEX-Upgrade: q-profile is clamped to the q_o=1 surface

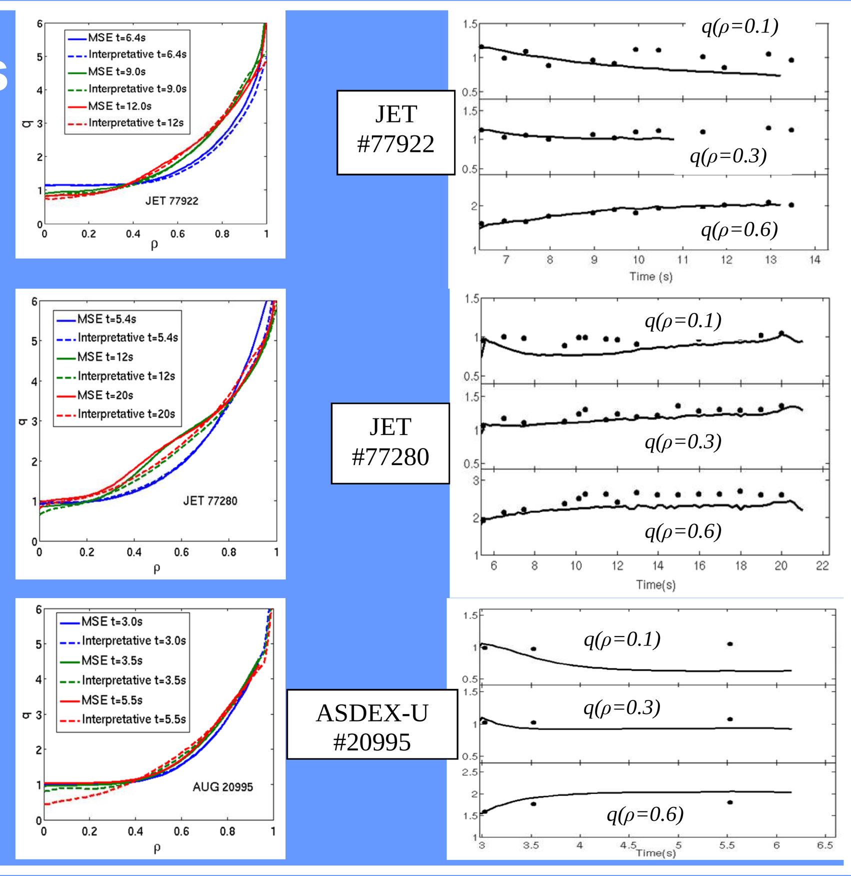

q-profile influence on transport [6]

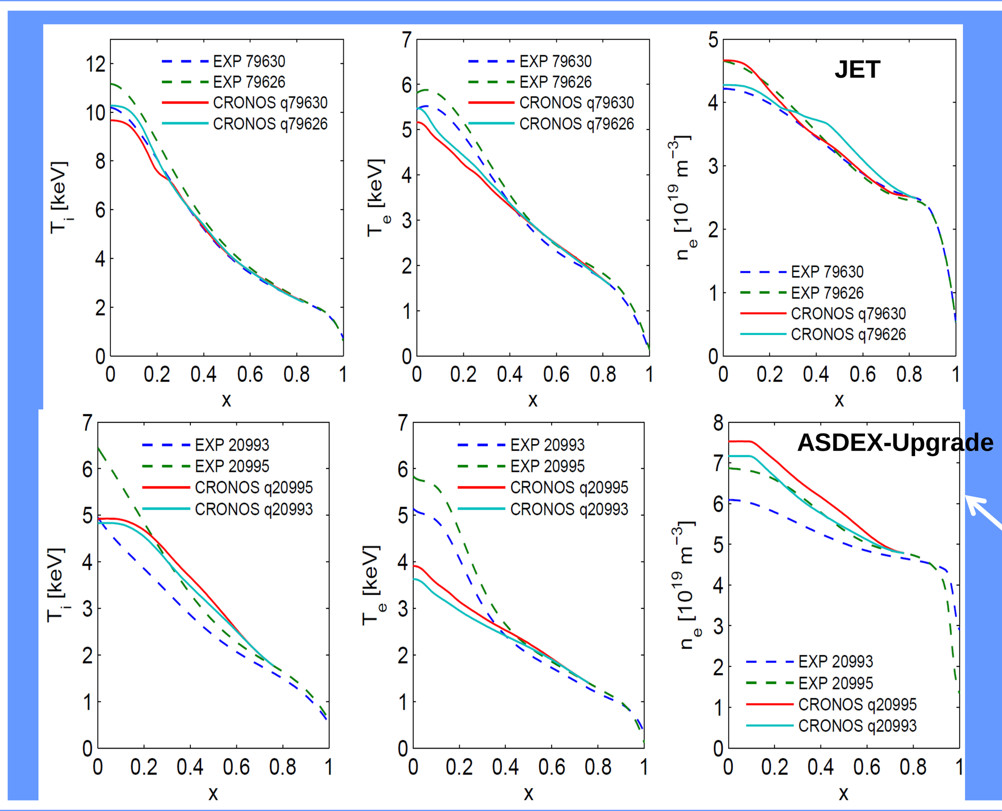

- Observed improved confinement partly explained by the q-profile modification maximising *s/q* ratio in the outer part of the plasma region which accounts for ~60-90% and ~35-55% of the observed ~20% confinement improvement in JET and ASDEX-Upgrade correspondingly [6].

Results of combined heat and particle transport GLF23 simulations for JET (top) and AUG (bottom) without ExB stabilisation effect. (left column) T_i profiles. (center column) T_e profiles. (right column), n_e profiles. (top): JET 79630, comparing q-profile inputs from both 79630 and 79626. (bottom) AUG 20995, comparing q-profile inputs from both 20995 and 20993.

- Core thermal energy in MJ following GLF23 predictions for JET and AUG hybrids.

Machine	pulses	Exp. [MJ]	Heat transport modeling [MJ]		Heat & particle transport modeling [MJ]	
			no ExB	with ExB (α_E=1.35)	no ExB	with ExB
JET	79626	1.97	1.9	2.62	1.83	3.03
	79630	1.67	1.71	2.37	1.71	2.68
AUG	20995	0.294	0.293	0.421	0.3	0.429
	20993	0.2	0.249	0.367	0.255	0.371

Self-consistent modelling of hybrid scenario (current, thermal, particle and rotation): ExB shear influence on transport [8,9]

- Validation of the GLF23 transport models in the self-consistent four-field: density, temperatures and momentum + first application of the TGLF model
- GLF23 : good agreement with measured density by reducing α_E by factor 2 – Te & Ti well predicted
- ASTRA [7] simulations of toroidal rotation using the GLF23 [8,9]:
  - GL23 momentum transport strong over-prediction of toroidal rotation
  - A better agreement with measured toroidal velocity when applying the fraction of the GLF23 computed thermal ion diffusivity for momentum transport.
  - The Prandtl number is P_r=0.3 and P_r=0.5 in low and high triangularity discharges

ASTRA simulations with GLF23 (blue curves) and TGLF (red curves) models performed with α_E=0.5 and P_r = 0.5 for JET high triangularity hybrid

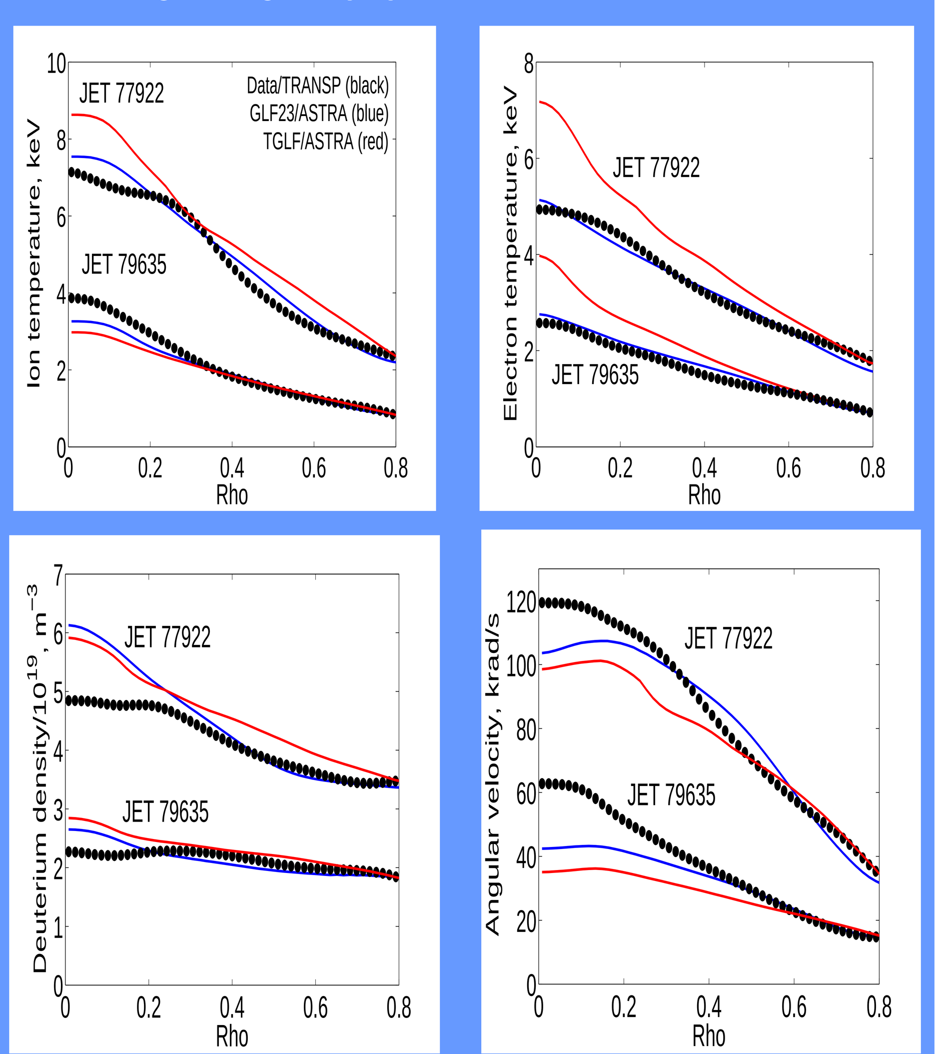

Modelling of hybrid termination

- Simulation (density, T_e and T_i evolution) of termination of JET hybrid scenarios including the H-L transition + Ip and Bo ramp down phase
- The transition from hybrid performance with type I ELMs to type III reproduced with the Bohm-gyroBohm model and continuous ELM model by reducing the ballooning stability limit and L-H threshold power by 40%.
- transition from type III H-mode to ohmic plasma with the reduction of power below the L-H threshold by switching from the H-mode to L-mode Bohm-gyroBohm model

JET #77922: (left) NBI power, D_α, thermal electron energy, central line averaged density, volume averaged ion temperature; (right) measured (High Resolution Thomson Scattering) and simulated n_e and T_e profiles. Measurements (blue) and simulations (red)

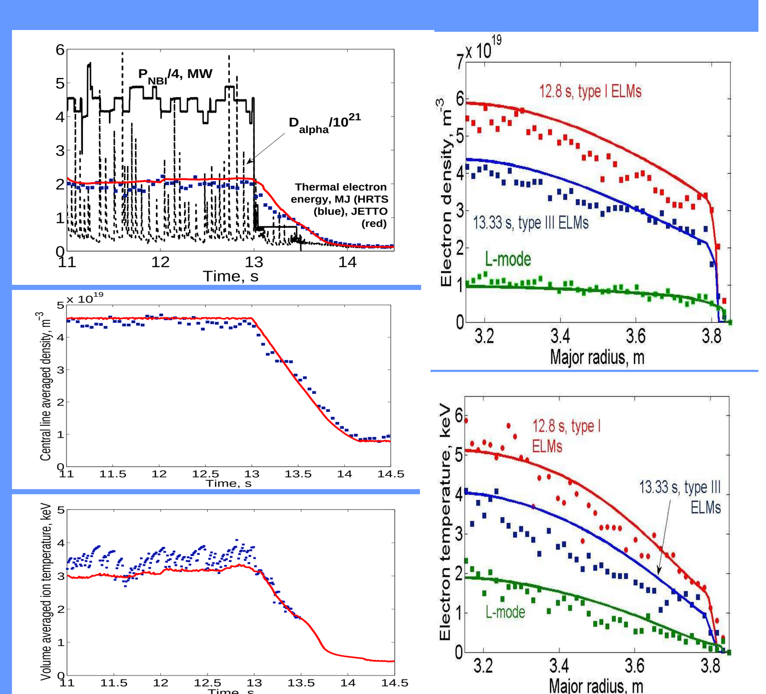

Self-consistent current, temperature and density JETTO modelling during the L-mode ramp down phase.

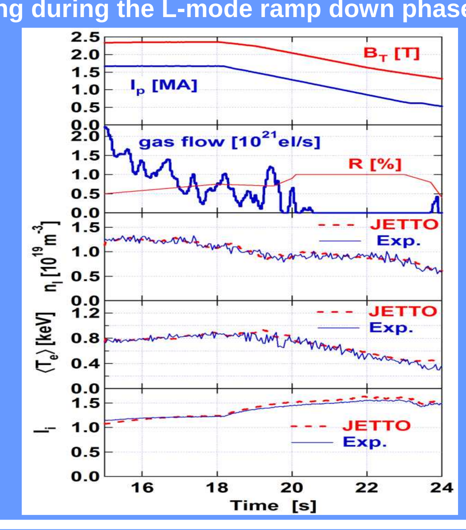

Task Force on Integrated Tokamak Modelling

EFDA — EUROPEAN FUSION DEVELOPMENT AGREEMENT

Predictive integrated modeling of ITER hybrid scenario (see also Parail V. et al this conference)

ITER hybrid operational domain from 0-D modeling

- simulations performed with the 0.5-D code METIS [10]
- fast calculation in order to scan the operational domain
- double constrain $q_0>1$ for 1000s and $Q_{DT}>5$
- $Ip=12MA$ at $B_T=5.3T$ ($q_{95}=4.3$), with the ITER baseline heating mix 20MW ICRH, 33MW NBI, 20MW ECCD and with a line averaged density fixed to $n_l=7.5\times10m^{-3}$ ($n_l/n_{Gw}\sim0.8$) during the burn phase

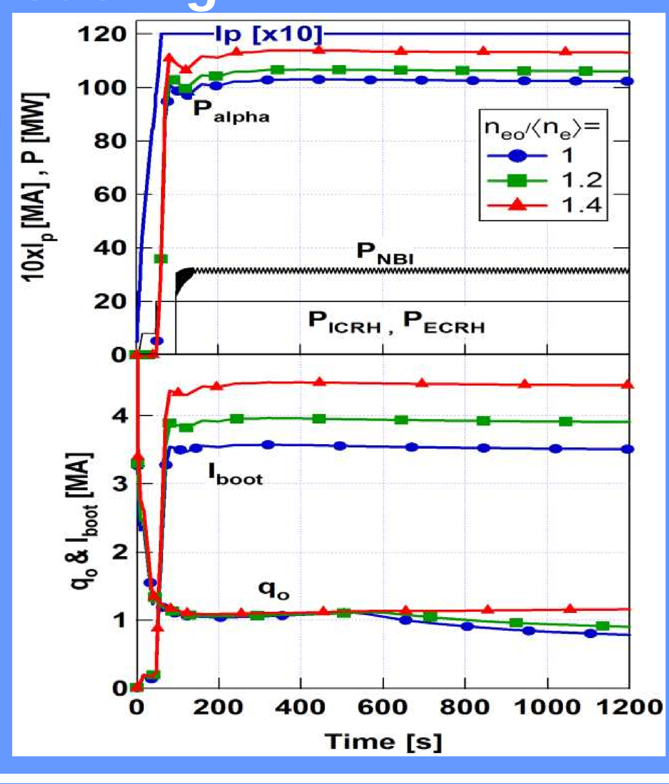

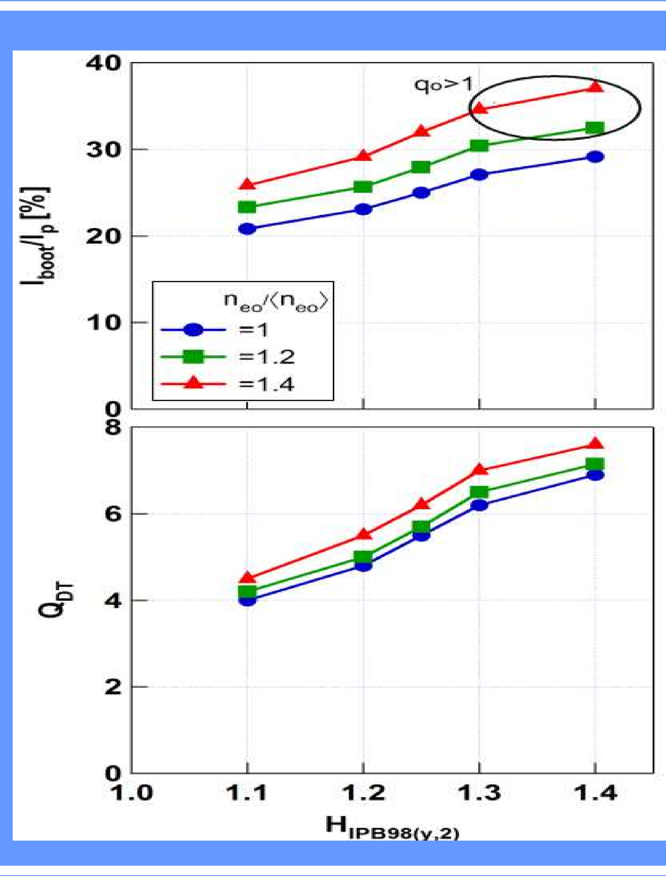

- sensitivity study are the density peaking factor with $n_{eo}/n_l=1,1.2,1.4$ and $H_{98IPB(y,2)}\sim1.1, 1.2, 1.25, 1.3, 1.4$
- METIS calculations indicate that high confinement and peaked density profiles are required to increase the bootstrap current at level above a certain value ($I_{boot}\sim4MA$ or $I_{boot}/I_p\sim30\%$) to sustain the q-profiles above unity

Current profile optimization during current ramp-up phase [11,12,13]

- ✓ q profile with $q_0>1$ at the end of the current ramp up phase with the ITER heating systems
- ✓ The flexibility of the heating system open the route to an active control of the q-profile
- ✓ Optimum between resistive flux consumption Ejima coefficient, C_E and optimizing the q profile $F=\langle s/q \rangle\, q_a$

Sensitivity studies :

(i) with and without Ip overshoot,
(ii) with early heating,
(iii) with or without early H-mode transition,
(iv)with different assumptions on density peaking,
(v) edge temperature,
(vi) effective charge.

Assumptions for reference case:

(i) Simulations start 1.5s after breakdown, when $I_p=0.5MA$. Current flat top (12MA) at 80 s with an expanding elongated shape, starting on the Low Field Side (X-point at 15s $I_p=3.5MA$).

(iii) The parabolic density profile with $n_{eo}/\langle n_e\rangle=1.3$ and $n_e=0.25xn_{eGw}$

(ii) A flat Z_{eff} profile, decreasing in time from 5 to 1.7

(iv) An L-mode edge with applied power (after 50s) below the L-H power threshold (~29MW).

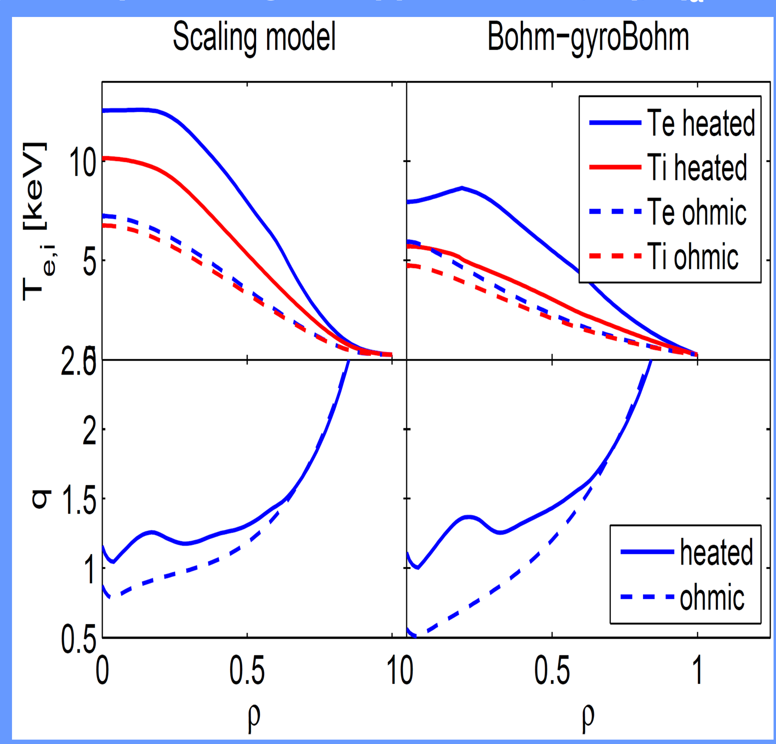

Te,i and q profiles for the optimized L-mode current ramp-up scenario with current flat top 12MA at 80s. For comparison, the profiles without any additional heating are also shown (dashed lines).

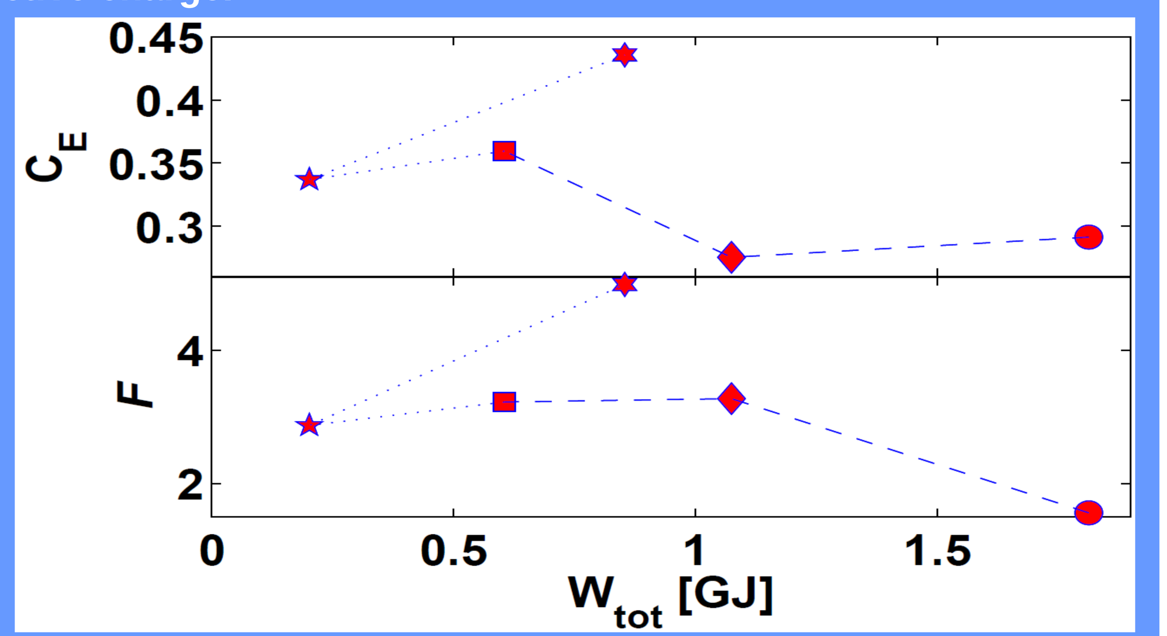

C_E and q-profile figure of merit, F, at the end of the 12MA ramp-up phase for the reference case on Fig 8 (square), the examples with early heating at 30s (diamond), with transition to H-mode at 55s (circle), with fast current ramp 12MA at 60s (pentagram), with a 10s/14MA current overshoot (hexagram

Pedestal prediction with first principle predictive model EPED [14,15]

✓ EPED is a first-principle model for predicting the H-mode pedestal height and width two constraints: (1) onset of non-local peeling–ballooning modes at low to intermediate mode number, (2) onset of nearly local kinetic ballooning modes at high mode number.

- Input : $B_t(T)$, $I_p(MA)$, $R(m)$, $a(m)$, δ, κ, $n_{e,ped}$ ($10^{19}m^{-3}$), Z_{eff}, β_N
- Scan : I_p=11, 12, 13MA , Z_{eff}=1.7, 2.5 , $n_{e,ped}$=6.5, 7.5, 8.5, 9.5, 10.5x$10^{+19}m^{-3}$ β_N =1.8, 2.2, 2.6, 3.0

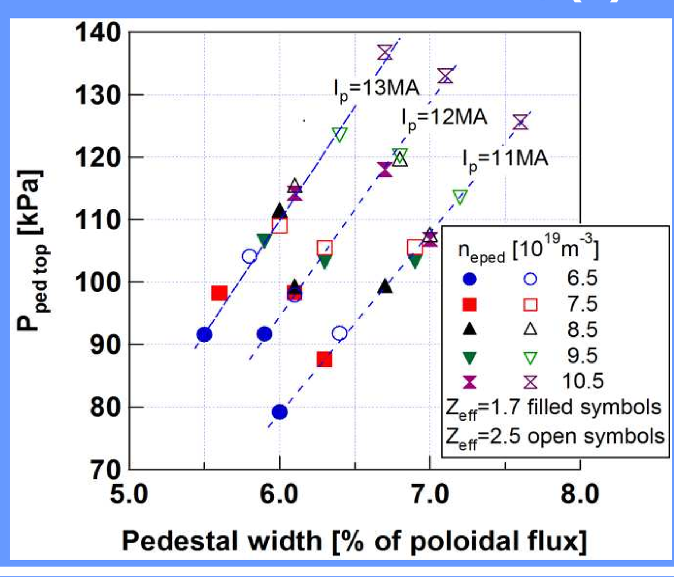

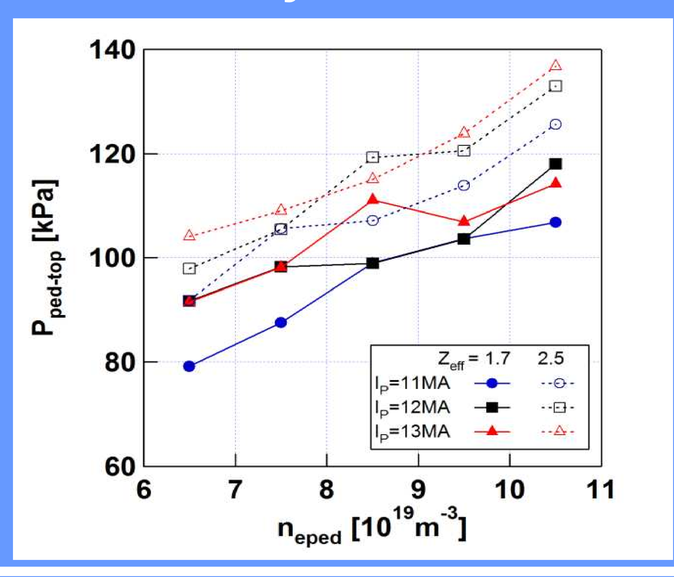

- weak dependence with β_N
- pedestal height increases with density (collisionality dependence of the kink/peeling stability limit)

Consistent core and pedestal integrated modeling

- CRONOS simulation: GLF23 (core) with EPED constrains
- Prescribed density profile scan at fixed
  - $n_l=8.8\times10^{19}m^{-3}$ and $n_{eo}/n_l=1,1.25,1.5$
  - consistent core & edge simulations n_{eo}/n_l ↑ at n_l=cst:
    - Edge confinement ↓
    - Core confinement ↑

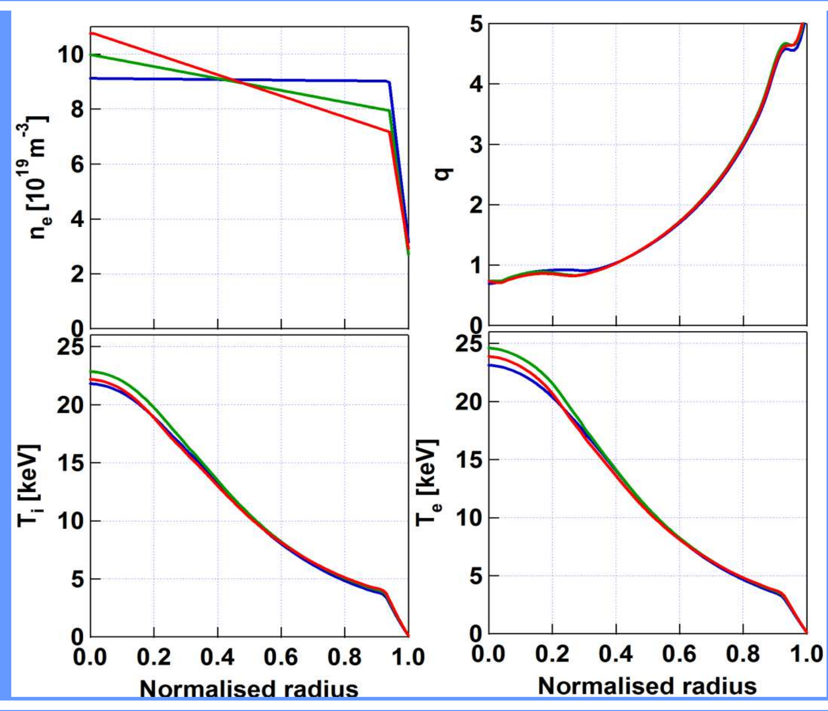

- CRONOS modelling of ITER hybrid scenario with GLF23 + pedestal parameters calculated with EPED

n_{eo}/n_l	$n_{e,top}$ [$10^{19}m^{-3}$]	$T_{i,top}$ [keV]	P_{top} [kPa]	Δ_{top} [ψ_{norm}]	Q	I_{boot}/I_P	β_N	$H_{IPB98(y,2)}$
1	9.02	3.67	96.3	0.064	4.71	30%	1.91	1.06
1.25	7.99	3.9	90.2	0.064	5.06	33%	1.97	1.08
1.5	7.24	4.02	84.4	0.064	5.06	33%	1.93	1.05

Model-based Magnetic and Kinetic real time Control [17-19]

- An integrated model-based plasma control strategy, ARTAEMIS [21, 22] applied to ITER hybrid regime for the control of the poloidal flux profile and P_α . The control actuators are NBI, ECRH, ICRH and LHCD systems, and the plasma surface loop voltage.
- The nonlinear plasma response to the actuators is modeled with METIS. A two-time-scale model identified from open-loop simulations.
- Closed-loop control simulations were performed by inserting the METIS code at the output of the two-time-scale ARTAEMIS controller. Various target profiles for the poloidal flux have been obtained simultaneously with various target levels of fusion power. This shows that current profile control can be combined with burn control, sharing a common set of actuators.

[1] Falchetto et al P2-25 this conference (2012) , Kalupin et al P2-01 this conference (2012)
[2] Joffrin E et al 2010 Proc. 23rd Int. Conf. on Fusion Energy 2010 (Daejeon, South Korea 2010) (Vienna: IAEA)
[3] Hobirk J et al Plasma Phys. Control. Fusion 54 (2012) 095001
[4] Stober J et al Nucl. Fusion 47 (2007) 728
[5] Artaud J.F. et al, Nucl. Fusion 50 (2010) 043001
[6] Citrin J. et al, Plasma Phys. Contr. Fusion 54 (2012) 065008
[7] Pereverzev G.V., Yushmanov P.N. 2002 Report IPP 5/98, Max-Planck-Institute fur Plasmaphysik
[8] Voitsekhovitch I. et al., in Proc. 39th EPS Conf on Plasma Physics and 16th International Congress on Plasma Physics (Stockholm, Sweden, 2012), Vol. 36F file P4.066 (2012)
[9] Voitsekhovitch et al, Nucl. Fusion 49 (2009) 055026
[10] Artaud J.F. et al, in proc 32nd EPS Conf., (Spain, Tarragona, 2005) ECA Vol. 29C, P1.035 (2005)
[11] Hogeweij G.M.D. et al, Plasma & Fus Res. 7 (2012) 2403063 and sub to Nuc. Fusion
[12] Imbeaux F. et al, Nucl. Fusion 51 (2011) 083026
[13] Voitsekhovitch I. et al Plasma Phys. Contr. Fusion 52 (2010) 105011
[14] Snyder P.B. et al Nucl. Fusion 51 (2011) 103016
[15] Snyder P.B et al Phys. Plasmas 19 (2012) 056115
[16] Citrin J. et al, Nucl. Fusion 50 (2010) 115007
[17] Moreau D. et al., Nucl. Fusion 48 (2008) 106001 and Nucl. Fusion 51 (2011) 063009
[18] Moreau D. et al., 2012, 24th IAEA Fusion Energy Conference, paper ITR/P1-20
[19] Liu F. et al., in Proc. 39th EPS Conf (Stockholm, Sweden, 2012), Vol. 36F file P1.063 (2012)

Acknowledgement: This work, supported by the European Communities under the contracts of Association between EURATOM and CEA, CCFE, IST, FOM, IPP, ÖAW, TEKES was carried out within the framework of the Task Force on Integrated Tokamak Modelling of the European Fusion Development Agreement. The views and opinions expressed herein do not necessarily reflect those of the European Commission